IEEE Open Journal of Vehicular Technology

Received 15 August 2023; accepted 8 September 2023. Date of publication 22 September 2023;
date of current version 23 October 2023. The review of this article was coordinated by Editor Symeon Chatzinotas.

Digital Object Identifier 10.1109/OJVT.2023.3316117

Comparing Aerial-RIS- and Aerial-Base-Station-Aided Post-Disaster Cellular Networks

MAURILIO MATRACIA [1] (Student Member, IEEE), MUSTAFA A. KISHK [2] (Member, IEEE), AND MOHAMED-SLIM ALOUINI [1] (Fellow, IEEE)

[1]Computer, Electrical, and Mathematical Sciences and Engineering (CEMSE) Division, King Abdullah University of Science and Technology (KAUST), Makkah 23955, Kingdom of Saudi Arabia
[2]Electronic Engineering Department, Maynooth University, W23 F2H6 Maynooth, Ireland

CORRESPONDING AUTHOR: MAURILIO MATRACIA (e-mail: maurilio.matracia@kaust.edu.sa)

ABSTRACT Reconfigurable intelligent surface (RIS) technology and its integration into existing wireless networks have recently attracted much interest. While an important use case of said technology consists in mounting RISs onto unmanned aerial vehicles (UAVs) to support the terrestrial infrastructure in post-disaster scenarios, the current literature lacks an analytical framework that captures the networks' topological aspects. Therefore, our study borrows stochastic geometry tools to estimate both the average and local coverage probability of a wireless network aided by an aerial RIS (ARIS); in particular, the surviving terrestrial base stations (TBSs) are modeled by means of an inhomogeneous Poisson point process, while the UAV is assumed to hover above the disaster epicenter. Our framework captures important aspects such as the TBSs' altitude, the fact that they may be in either line-of-sight or non-line-of-sight condition with a given node, and the Nakagami-*m* fading conditions of wireless links. By leveraging said aspects we accurately evaluate three possible scenarios, where TBSs are either: *(i)* not aided, *(ii)* aided by an ARIS, or *(iii)* aided by an aerial base station (ABS). Our selected numerical results reflect various situations, depending on parameters such as the environment's urbanization level, disaster radius, and the UAV's altitude.

INDEX TERMS RIS, UAV, coverage probability, stochastic geometry, post-disaster communications.

I. INTRODUCTION

Natural and human-made disasters are extreme events that can potentially compromise the life and economy of any affected region. According to the Institute for Economics and Peace (IEP), the overall frequency of natural disaster has increased by approximately ten times during the last sixty years [1], especially due to the recent rise of climate change. Just in 2021, 432 natural calamities (responsible for 10,492 deaths and 252 billion USDs) have been reported by the Emergency Event Database (EM-DAT) [2]. In addition, recent conflicts such as the one between Russia and Ukraine, as well as the serious terrorist attacks occurred in Sub-Saharan Africa and the Middle East cannot be overlooked. On the bright side, we should also recall that the improved safety measures and the ease of relocating to safer places often succeeded in limiting the number of human deaths: while for natural disasters it has significantly decreased over the last century [1, Fig. 3.5], over the year 2021 the lethality of terrorist attacks declined from 1.6 to 1.4 deaths per event [3, Executive Summary].

However, one of the main issues faced in search and rescue (SAR) missions is the lack of reliable and ubiquitous connectivity, which prevents first responders from properly coordinate and support victims. In fact, conventional telecom infrastructures are based on cell towers, which are generally susceptible to strong perturbations as well as power outages. Hence, during the last decade many researchers have investigated potential solutions such as the ones based on the deployment of aerial nodes. In particular, despite their limited endurance and payload capability, unmanned aerial vehicles (UAVs) probably represent the most promising technology due to advantages such as safety (because no persons are onboard), low cost, quick deployment, and relocation flexibility.

While most of the studies in this field focused on the possibility of mounting radio frequency (RF) transceivers on UAVs, a more recent solution consists in using reconfigurable intelligent surfaces (RISs), also referred to as intelligent reflective surfaces (IRSs), instead of cellular transceivers. The main differences between these two options can be summarized as follows:

- While RF transceivers are already available on the market, RISs are still at the prototyping stage;
- RF transceivers are active elements, while RISs can be considered as passive ones. Therefore, ARISs are expected to be much more energy-efficient than ABSs (also thanks to novel optimization alghorithms such as the one proposed in [4]);
- The powers received from an RIS and a BS follow different channel models, as clarified in Section II.

Keeping these aspects in mind, in this work we try to make a fair comparison between the UAV-mounted base station (BS) and UAV-mounted RIS paradigms in typical post-disaster scenarios.

A. RELATED WORKS

In this subsection, we will provide a brief summary of the relevant and recent literature works that have focused on either terrestrial or UAV-aided post-disaster wireless networks. For a more comprehensive literature overview the reader can refer to our survey [5].

1) TERRESTRIAL SOLUTIONS

Not many recent studies have focused on terrestrial wireless networks in emergency situations. However, our recent work [6] presented a novel interference mitigation strategy based on location-dependent silencing. By means of numerical results, we proved that a proper implementation of such strategy leads to significant improvements of both the average coverage probability and signal-to-interference-plus-noise (SINR) meta distribution, which allows to quantify the wireless links' reliability.

Another important technology that can be exploited in post-disaster scenarios is the device-to-device (D2D) paradigm, which was suggested by authors in [7] for networks in inband overlay mode, by modeling the aggregate interference and SINR distribution by means of marked PPPs. Finally, it is worth mentioning [8] for having suggested the concept of ground vehicle-mounted base stations, called movable and deployable resource units (MDRUs).

2) UAV-MOUNTED BSS

Another interesting topic is the use of UAV-mounted base stations (BSs) in post-disaster scenarios, which has been considered in relevant works such as [9], [10], [11]. In particular, authors in [9] suggested a fleet consisting of a tethered drone for high-capacity backhauling, an untethered drone for coverage, and an untethered powering drone to charge the former. Furthermore, an interesting study on post-disaster networks was presented in [10], which assumed multiple areas of failure with random size and therefore implemented specific Poisson cluster processes (PCPs) in order to derive not only the downlink (DL) coverage probability, but also energy efficiency and spectral efficiency.

Finally, in [11], we have modeled the VHetNet resulting from the occurrence of a calamity by means of the binomial point process (BPP) and the inhomogeneous Poisson point process (IPPP), respectively for the aerial and terrestrial BS tiers; in this way, we could accurately evaluate the performance of the network depending on several parameters, such as the entity of the ad hoc aerial fleet, size of the disaster, and distance from the disaster epicenter.

3) UAV-MOUNTED RISS

Given that ARISs are the main focus of this article and there are not many works considering this paradigm for emergency scenarios, for this topic we will provide a broader overview of the relevant literature.

Authors in [12] presented a novel network architecture where an ARIS is used to achieve better coverage compared to its terrestrial counterpart; to do this, the authors jointly optimized the transmit beamforming of the source node, as well as the ARIS' placement and phase shifts. Similarly, authors in [13] considered an ARIS assisting a millimiter-wave (mmWave) BS, and proposed an algorithm to minimize the UAV's energy consumption. Furthermore, the study presented in [14] focused on using the ARIS technology within the terahertz (THz) band, for which a higher number of antenna elements can be installed on the ARIS compared to conventional wireless communications frequency bands; the authors took into account multiple aspects (including the transceiver-RIS distances, blockage probability, and size of the RIS) to search for the optimal deployment in terms of throughput. Furthermore, authors in [15] investigated the gain that a drone-mounted RIS can provide when supporting a HAP-mounted BS that covers a given area on the ground; to this extent, both the trajectory and phase-shift of the ARIS were jointly optimized, leading to significant improvements in terms of received SNR.

In the context of public safety networks, the authors of [16] investigated the network performance for search and rescue (SAR) missions when deploying a UAV-mounted IRS; in particular, the authors focused on the data rate as a function of the UAV's altitude and distance from the closest TBS, but without taking into account the interference coming from any other BSs. Moreover, authors in [17] considered a fixed-wing UAV (since, compared to its rotary-wing counterpart, it is capable of carrying a larger RIS) serving trapped users, and assumed Fisher-Snedecor-F composite fading conditions; the study provided novel closed-form expressions for the channel statistics, achievable rate, outage probability, and bit error rate. Finally, the reader can refer to [18] for an overview of

the potential ARISs' use cases depending on the type of aerial vehicle.

B. CONTRIBUTIONS

This article contributes in multiple ways to the existing literature, as explained in the following lines.

1) SYSTEM MODEL

In our novel setup, we assume a large-scale post-disaster wireless network including a region that is affected by a calamity. Due to this, the intra-region TBSs are modeled as an inhomogeneous PPP (IPPP) which captures their quality of resilience (QoR) to the disaster. To make up for the failures of some of the TBSs and improve the connectivity for both victims and first responders within the disaster-struck area, an ad hoc UAV carrying either an RIS or a BS is deployed above the epicenter.

2) PERFORMANCE ANALYSIS

In this article, we borrow tools from stochastic geometry (SG) to fairly compare three types of post-disaster networks (the terrestrial-only, ARIS-aided, and ABS-aided ones) in terms of local and average coverage probabilities. To the best of our knowledge, no work in the literature has ever done this; hence, the expressions of the minimum distance distributions, association probabilities, Laplace transforms of the interference, and coverage probabilities derived in Section III are all novel.

3) SYSTEM-LEVEL INSIGHTS

By properly selecting the system parameters and inspecting the behaviors of the consequent local and average coverage probabilities, we are able to extract fruitful insights. For example, the obtained results show that, while the ARIS is almost always the best solution to improve coverage in emergency scenarios, the benefits it can provide strongly depend on its altitude, number of elements, and urbanization level of the environment.

C. ORGANIZATION OF THE PAPER

The structure of this manuscript's remainder can be summarized as follows.

- In the next section we describe both the network model (by illustrating and explaining the considered network architecture) and channel model (by defining all the metrics of interest);
- In the core sections of the paper, Sections III and IV, we respectively develop our analytical framework and use it to investigate how the local and the average coverage probabilities depend on the various system parameters;
- Finally, in Section V we summarize the article, draw our conclusions, and envision potential extensions of our study.

II. SYSTEM MODEL

A. NETWORK MODEL

The considered network model is characterized by a disaster-struck area $\mathcal{A}_d$ (of circular shape and with radius r_d) where the cellular infrastructure is damaged. For simplicity and without any loss of generality, the origin $\boldsymbol{O}$ is set at the center of $\mathcal{A}_d$. Moreover, we assume that all TBSs have height h_T, and the surviving ones are modeled by means of the IPPP $\Phi \equiv \{W_i\} \subseteq \mathbb{R}^2$ of intensity $\lambda(r) = \lambda_0 \left(\chi(r)\, \mathbb{1}(r \leq r_d) + \mathbb{1}(r > r_d)\right)$, where the terms $\lambda_0 \geq 0$, $r \geq 0$, and $\chi(r) \in [0, 1]$ denote the original TBS density, the ground distance from the origin, and terrestrial infrastructure's QoR, respectively. Finally, we consider the possibility of deploying an ad hoc UAV carrying either an RIS or a BS at altitude h_A above the disaster epicenter, in order to make up for the failure of some of the TBSs (see Fig. 1).

Now, results such as the ones proposed in [19, Fig. 5] showed that non-line-of-sight (NLoS) links usually have negligible influence on networks' performance, because of the huge path losses they are subject to; therefore, for the sake of both conciseness, readability, and tractability, we restrict our analysis only to the line-of-sight (LoS) wireless links and assume no correlation between the TBSs seen by the typical user equipment (UE) and the ones seen by the UAV. Moreover, we introduce a specific notation for different types of TBSs, in accordance with Table 1 (where Q denotes the average received power and W the location of the TBS). Finally, we assume that the RIS is configured in a way that allows to isolate the signal coming from the serving TBS and accurately reflect it to the intended UE; therefore, the interference due to indirect paths can be neglected.

B. CHANNEL MODEL

In this study, we assume that all TBSs transmit their signals with the same constant power ρ. We also assume that the probability of LoS between a ground user and any other node follows the model proposed in [20][1]; hence, it can be expressed as

$$\mathcal{P}_L(r, h) = \left(1 + \frac{\mathcal{S}}{\exp\left(\mathcal{S}'\left(\frac{180}{\pi}\arctan\frac{h}{r} - \mathcal{S}\right)\right)}\right)^{-1}, \quad (1)$$

where $\mathcal{S}$ and $\mathcal{S}'$ are referred to as *s-curve* parameters (which depend on the urbanization level of the environment), r is the horizontal distance between the UE and the other node, and h is the altitude of the latter. However, this model should not be applied when both the considered points are considerably above the ground, because in that case there is a significantly less density of potential obstructions. Therefore, we fairly assume that all TBSs are in LoS with the UAV[2], and hence

[1] Although this model was originally introduced to model the LoS probability between an aerial and a terrestrial node, since it is based on environmental and purely geometrical aspects it can also be applied for the case when both nodes are terrestrial, as already done in [21, Sec. V] for example.

[2] For a more accurate (but less tractable) characterization, the reader can refer to [20, Eq. (4)].

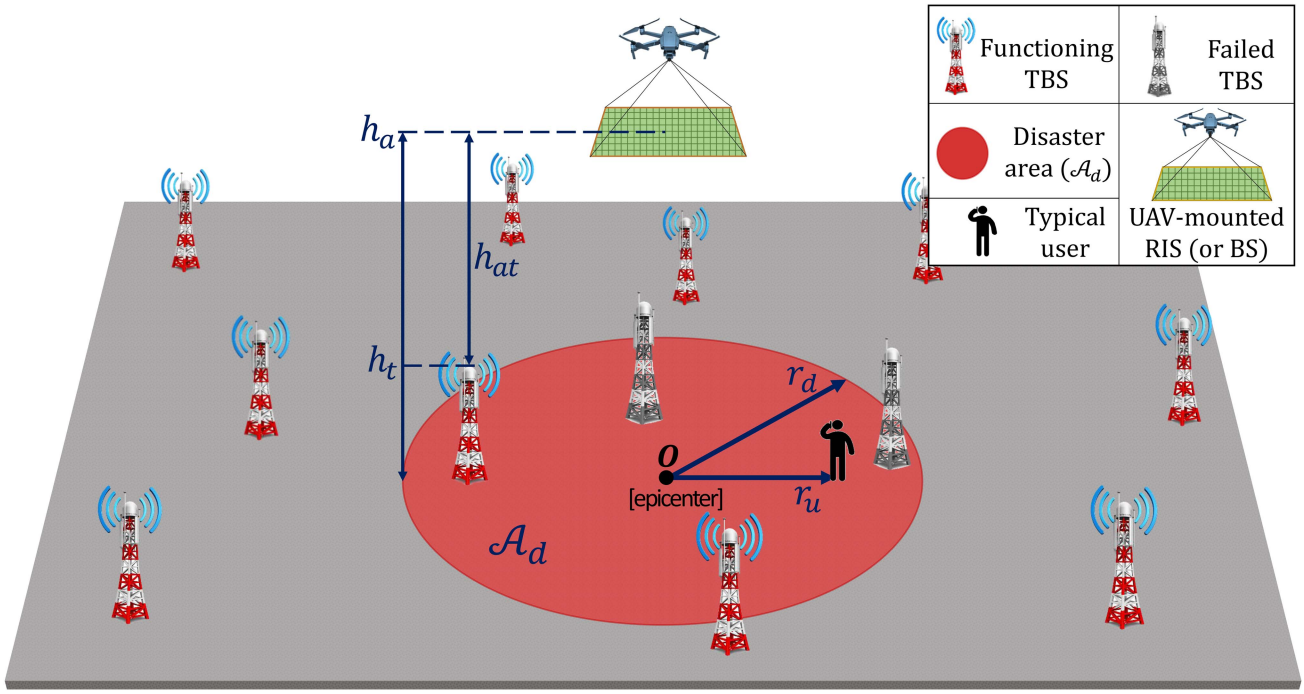

FIGURE 1. Schematic representation of the system setup: the typical UE is located at distance r_u from the origin, all the failed TBSs belong to a circular disaster-struck region $\mathcal{A}_d$, and an ad hoc UAV-mounted RIS (or BS) is deployed at altitude h_A above the disaster epicenter. All TBSs' heights are assumed equal to h_T.

TABLE 1. Main Subscripts

Notation	Description	Definition
ϱ	ARIS	—
b	ABS	—
A	Either ARIS or ABS	$\varrho \oplus b$
T	Functioning TBSs in LoS with the typical UE	—
O	Any type of relevant node	$\varrho \oplus b \oplus T$
B	Type of serving node	$B \in \{r, b, T\} \ \wedge \ Q_{B,W^*} > Q_{O,W^*}, \ \forall O \neq B$

we can consider ideal backhaul link for the ABS (this would actually be realistic, at least in terms of SIR, whenever TBSs transmit backhaul signals with very narrow beams). Finally, let us define the NLoS probability as $\mathcal{P}_N(r, h) = 1 - \mathcal{P}_L(r, h)$.

By taking into account the mean loss coefficient η (which also depends on the type of environment), the effective power would be equal to $\xi = \eta\,\rho$; however, by considering only the user's LoS-TBSs (LTBSs) and neglecting the noise power σ_n^2, [3] we henceforth normalize the effective power to 1. All the LoS links experience Nakagami-m distributed fadings (with shape parameter defined as m), and the signals propagate according to the standard power-law model with path loss exponent $\alpha \geq 2$.

[3] To justify these simplifications we highlight that, according to our tests, the sum of the aggregate NLoS interference and the noise power generally accounts for less than 1% of the aggregate LoS interference.

Let $\Gamma(m) = \int_0^\infty x^{m-1}\, e^{-x}\, \mathrm{d}x$ denote the Gamma function, then the channel fading power gains of all links follow a Gamma distribution with probability density function (PDF) given as

$$f_G(g) = \frac{m^m\, g^{m-1}}{\Gamma(m)}\, e^{m\,g}. \tag{2}$$

C. RECEIVED POWERS AND ASSOCIATION POLICY

Let r_u denote the distance of the typical user from the disaster epicenter. Then, the instantaneous received power coming from a functioning BS transmitting to the user through a direct LoS path is

$$q_b = G_b\, \left(r_u^2 + h_A^2\right)^{-\frac{\alpha}{2}}, \tag{3}$$

if the BS is aerial, and

$$q_{T,W_i}(\Omega) = G_{T,W_i}\, \left(\Omega^2 + h_T^2\right)^{-\frac{\alpha}{2}}, \tag{4}$$

if it is terrestrial, where Ω denotes the random horizontal distance between the UE and W_i, and G_{T,W_i} is the fading gain experienced by the corresponding LTBS-UE wireless link. On the other side, the power received by the typical UE through an ARIS via indirect LoS path can be generally expressed by adopting the product-distance path loss model [22, Sec. II-A]

$$q_{\varrho,W_i}(R) = M^2\, G_\varrho\, (r_u^2 + h_A^2)^{-\frac{\alpha}{2}}\, G'_{\varrho,W_i}\, (R^2 + h_{AT}^2)^{-\frac{\alpha}{2}}, \quad (5)$$

where M denotes the RIS' number of elements, R refers to the random horizontal distance between the ARIS and its closest TBS, and $h_{AT} = h_A - h_T$; moreover, the fading gains G_ϱ and G'_{ϱ,W_i} respectively refer to the ARIS-UE and TBS-ARIS LoS paths.

We hereby adopt the maximum-average-received-power association rule. In other words, the typical user connects to the TBS that (either directly or indirectly), on average, provides the strongest received power; similarly, the ARIS selects the TBS providing the strongest received power (on average) and reflects the desired signal towards the UE. Given that for a given type of channel (corresponding to either a direct or indirect path) the only variable is the horizontal distance, the tagged TBS is always the closest among the ones of the same type. However, it is also possible to have interferers providing higher received powers at a given instant. Since we assume the fading gains' expected values equal to 1, the average powers received from LoS TBSs, ABS, and ARIS can be expressed as $\hat{q}_T(\Omega) = (\Omega^2 + h_T^2)^{-\frac{\alpha}{2}}$, $\hat{q}_b = (r_u^2 + h_A^2)^{-\frac{\alpha}{2}}$, and $\hat{q}_\varrho(R) = M^2\,((r_u^2 + h_A^2)\,(R^2 + h_{AT}^2))^{-\frac{\alpha}{2}}$, respectively.

D. SIGNAL-TO-INTERFERENCE RATIO (SIR)

Given that in large scale wireless networks the noise power is usually negligible compared to the power of the aggregate interference, we hereby restrict our interest to the signal-to-interference ratio (SIR). Recalling from Table 1 that B denotes the type of the tagged node and letting Q_{B^*} indicate the power received from it (either through direct or indirect path), the instantaneous SIR can be expressed as

$$\mathrm{SIR} = \frac{Q_{B^*}}{I_B}, \quad (6)$$

where

$$I_B = \begin{cases} \sum_{W_i \in \Phi_L} Q_{T,W_i} - Q_{B^*}\, \mathbb{1}(B = T), & \text{if } A = \varrho \\ \sum_{W_i \in \Phi_L} Q_{T,W_i} + Q_b - Q_{B^*}, & \text{if } A = b \end{cases}$$

indicates the aggregate interference affecting the UE in case of association to a node of type B (*i*.e., B-association), with $\Phi_L \subseteq \Phi$ being the IPPP describing the functioning LTBSs. Is should also be noted that, for the case when the user is served by the ARIS ($A = \varrho$), it is assumed that if the TBS serving the ARIS is also in LoS with the UE, then it always interferes destructively.

E. COVERAGE PROBABILITY

Our performance metric of interest is the coverage probability, which represents the complementary cumulative distribution function (CCDF) of the SIR evaluated at a certain threshold θ, which in turn corresponds to the minimum value that ensures reliable decoding; hence, the coverage probability can be expressed as

$$P_c = \mathbb{P}(\mathrm{SIR} > \theta). \quad (7)$$

III. PERFORMANCE ANALYSIS

This section preliminarily provides the mathematical expressions of the (i) distributions of distance to the closest LTBS from the UE's and the ARIS' perspectives, (ii) the probabilities that the user is served by a certain type of node, and (iii) the consequent conditional Laplace transforms of the aggregate interference through direct LoS paths. After having derived these terms, both the exact and approximate expressions of the coverage probability will be obtained by following the approaches proposed in [23] and [24], respectively.

A. DISTANCE DISTRIBUTIONS

The coverage probability strongly depends on the distance between the UE and the serving node. Since the distance between the UAV and the UE is deterministic, the lemmas presented in this subsection will only provide the distributions of the minimum horizontal distances of interest.

1) CLOSEST TBS SEEN BY THE ARIS

The following lemma provides the cumulative distribution function (CDF) of the distance to the closest TBS from the UAV-mounted RIS. Then, the respective PDF will be presented as a corollary.

Lemma 1: The CDF of the random horizontal distance Y between the ARIS and its nearest LTBS can be expressed as

$$F_Y(y) = 1 - \exp\left(-2\pi \int_0^y \lambda(r)\, r\, \mathrm{d}r\right). \quad (8)$$

Proof: The CDF of Y describes the behavior of the null probability [25] of the IPPP corresponding to all the surviving TBSs. Let $N(y)$ be the number of TBSs residing within a horizontal distance y from the origin, then:

$$\begin{aligned} F_Y(y) &= 1 - \mathbb{P}(Y > y) = 1 - \mathbb{P}\,(N(y) = 0) \\ &= 1 - \exp\left(-\int_0^{2\pi}\int_0^y \lambda(r)\, r\, \mathrm{d}r\, \mathrm{d}\vartheta\right), \end{aligned} \quad (9)$$

which is equivalent to (8).

Corollary 1: Henceforth, let the overline characterize the complementary functions (*i*.e., $\bar{F}_X(x) = 1 - F_X(x)$). Then, we can compute the PDF of the random variable (RV) Y as

$$f_Y(y) = 2\pi\, y\, \bar{F}_Y(y)\, \lambda(y). \quad (10)$$

Proof: The derivative of $F_Y(y)$ can be obtained as follows:

$$\begin{aligned} f_Y(y) = &-\exp\left(-2\pi \int_0^y \lambda(r)\, r\, \mathrm{d}r\right) \\ &\times \left(-2\pi\, \frac{\mathrm{d}}{\mathrm{d}y} \int_0^y \lambda(r)\, r\, \mathrm{d}r\right), \end{aligned} \quad (11)$$

where, by applying the Leibniz integral rule, the above derivative can be computed as

$$\frac{\mathrm{d}}{\mathrm{d}y}\int_0^y \lambda(r)\, r\, \mathrm{d}r = \lambda(r)\, r\, \frac{\mathrm{d}r}{\mathrm{d}y}\Big|_0^y + \int_0^y \frac{\mathrm{d}}{\mathrm{d}y}\lambda(r)\, r\, \mathrm{d}r = \lambda(y)\, y. \tag{12}$$

Noting that $\bar{F}_Y(y) = \exp(-2\pi \int_0^y \lambda(r)\, r\, \mathrm{d}r)$ completes the proof. ■

2) CLOSEST TBS SEEN BY THE TYPICAL UE

The following lemma provides the cumulative distribution function (CDF) of the distance to the closest TBS seen by the typical user. Next, a corollary will introduce the respective PDF.

Lemma 2: Henceforth, let (ω, β) be the polar coordinate system centered around the typical user; thus, the horizontal distance from the epicenter can be expressed as $r_\Omega(\omega, \beta) = \sqrt{r_u^2 + \omega^2 - 2 r_u\, \omega\, \cos(\beta)}$. By introducing the LTBSs' density $\lambda_L(r, h) = \lambda(r)\, \mathcal{P}_L(r, h)$, we can obtain the CDF of the horizontal distance Z between the user and the nearest LTBS as

$$F_Z(z) = 1 - \exp\left(-\int_0^{2\pi}\int_0^z \lambda_L\left(r_\Omega(\omega, \beta), h_T\right)\, \omega\, \mathrm{d}\omega\, \mathrm{d}\beta \right). \tag{13}$$

Proof: The CDF of Z can be derived by applying the same procedure seen in the proof of Lemma 1, thus is omitted. ■

Corollary 2: The PDF of the RV Z can be computed as

$$f_Z(z) = \bar{F}_Z(z)\, z\, \mathcal{P}_L(z, h_T) \int_0^{2\pi} \lambda\left(r_\Omega(z, \beta)\right)\, \mathrm{d}\beta. \tag{14}$$

Proof: The proof is similar to the one of Corollary 1, therefore is omitted. ■

B. ASSOCIATION PROBABILITIES

The B-association probabilities quantify the likelihood that the UE associates to a TBS through a specific path (*i*.e., direct, indirect via RIS, or indirect via ABS). In what follows, we study the cases when the tagged node is either an LTBS, an ARIS, or an ABS.

1) A-ASSOCIATION

When considering the association to the UAV, it should be noted that not only the TBS-UAV path, but also the UAV-UE path must be free from any obstruction. Keeping this in mind, the expressions of the association probability given that the UAV carries either an RIS or a BS is presented in the following theorem.

Theorem 1: Henceforth, let ζ denote the effective LoS ABS' transmit power normalized on its TBS' counterpart. By introducing $\mathcal{Z}_\varrho(y) = \sqrt{M^{-\frac{4}{\alpha}}\,(r_u^2 + h_A^2)\,(y^2 + h_{AT}^2) - h_T^2}$ and $\mathcal{Z}_b = \sqrt{\zeta^{-\frac{2}{\alpha}}\,(r_u^2 + h_A^2) - h_T^2}$, the A-association probability can be expressed as

$$\mathcal{A}_A = \begin{cases} \int_0^\infty a_\varrho(y)\, f_Y(y)\, \mathrm{d}y, & \text{if A} = \varrho \\ \mathcal{P}_L(r_u, h_A)\, \bar{F}_Z(\mathcal{Z}_b), & \text{if A} = \mathrm{b} \end{cases}, \tag{15}$$

where $a_\varrho(y) = \mathcal{P}_L(r_u, h_A)\, \bar{F}_Z(\mathcal{Z}_\varrho(y))$ denotes the conditional A-association probability, given that the UAV is carrying an RIS.

Proof: See Appendix A. ■

2) T-ASSOCIATION

The typical user will directly associate to the closest LTBS if the UAV is either: (i) in LoS with the UE but provides a weaker average received power, or (ii) in NLoS with the UE. Keeping this in mind, in the next theorem we provide the expressions of the T-association probabilities for the cases of ARIS and ABS deployments.

Theorem 2: Let $\mathcal{Y}_\varrho(z) = \sqrt{\frac{M^{\frac{4}{\alpha}}\,(z^2 + h_T^2)}{r_u^2 + h_A^2} - h_{AT}^2}$. Then, the T-Association probability can be computed as

$$\mathcal{A}_{T|A} = \begin{cases} \int_0^\infty a_{T|\varrho}(z)\, f_Z(z)\, \mathrm{d}z, & \text{if A} = \varrho \\ \mathcal{P}_L(r_u, h_A)\, F_Z(\mathcal{Z}_b) + \mathcal{P}_N(r_u, h_A), & \text{if A} = \mathrm{b} \end{cases}, \tag{16}$$

where $a_{T|\varrho}(z) = \mathcal{P}_L(r_u, h_A)\bar{F}_Y(\mathcal{Y}_\varrho(z)) + \mathcal{P}_N(r_u, h_A)$ expresses the conditional T-association probability when the ARIS is deployed.

Proof: See Appendix B. ■

C. CONDITIONAL LAPLACE TRANSFORMS OF THE INTERFERENCE

In this section, we will derive the expressions of the conditional Laplace transforms of the interference under the assumptions that all BSs share the same frequency or time resource blocks with a unit reuse factor. Moreover, since RISs are expected to accurately estimate the directions of the incoming signals and reflect them towards the intended users, it is fair to neglect the interference arriving at the UE through the RIS.

1) INTERFERENCE IN CASE OF A-ASSOCIATION

Based on the previously discussed assumptions, if the UE associates to the ad hoc aerial node, then the aggregate interference will be the sum of the instantaneous received powers coming from all the TBSs in LoS with the user (we hereby exclude the possibility of having constructive interference due to the same LTBS serving the user directly and indirectly at the same time). Therefore, the aggregate interference in case of A-association can be characterized by means of its Laplace transform, which is introduced in the following theorem.

Theorem 3: Given $A \in \{\varrho, b\}$ and recalling from Theorem 1 the expressions of $\mathcal{Z}_\varrho(y)$ and $\mathcal{Z}_b$, the Laplace transform of the interference in case of A-association can be

computed as either

$$\mathcal{L}_{\varrho}(s,y) = \exp\left(-\int_0^{2\pi}\int_{\mathcal{Z}_{\varrho}(y)}^{\infty} \lambda_L\left(r_{\Omega}(\omega,\beta),h_T\right) \times \mathcal{I}_T(s,\omega)\,\omega\,\mathrm{d}\omega\,\mathrm{d}\beta\right), \quad \text{if A} = \varrho, \tag{17}$$

or

$$\mathcal{L}_{b}(s) = \exp\left(-\int_0^{2\pi}\int_{\mathcal{Z}_{b}}^{\infty} \lambda_L\left(r_{\Omega}(\omega,\beta),h_T\right) \times \mathcal{I}_T(s,\omega)\,\omega\,\mathrm{d}\omega\,\mathrm{d}\beta\right), \text{if A} = \text{b}, \tag{18}$$

where, henceforth,

$$\mathcal{I}_T(s,\omega) = 1 - \left(\frac{m}{m + s\,(\omega^2 + h_T^2)^{-\frac{\alpha}{2}}}\right)^m. \tag{19}$$

Proof: See Appendix C. ■

2) INTERFERENCE IN CASE OF T-ASSOCIATION

For the case when the UE is directly served by an LTBS, the aggregate interference will be the sum of the instantaneous received powers coming from all the remaining LTBSs and (possibly) the ABS. Therefore, the expression of the corresponding conditional Laplace transform of the interference is presented in the following theorem.

Theorem 4: The Laplace transform of the interference in case of T-association can be computed as

$$\mathcal{L}_{T|A}(s,z) = \begin{cases} \mathcal{L}_{TT}(s,z), & \text{if A} = \varrho \\ \mathcal{L}_{TT}(s,z)\,\mathcal{I}_b(s), & \text{if A} = \text{b} \end{cases},$$

where

$$\mathcal{L}_{TT}(s,z) = \exp\left(-\int_0^{2\pi}\int_{z}^{\infty} \lambda_L\left(r_{\Omega}(\omega,\beta),h_T\right) \times \mathcal{I}_T(s,\omega)\,\omega\,\mathrm{d}\omega\,\mathrm{d}\beta\right) \tag{20}$$

and $\mathcal{I}_b(s) = \left(\frac{m}{m+s\,(r_u^2+h_A^2)^{-\frac{\alpha}{2}}}\right)^m$ describe the overall interferences coming from the LTBSs and ABS.

Proof: When $A = \varrho$, the aggregate interference is just the sum of the instantaneous received powers coming from the LTBSs, because the interference coming from the ARIS is null; then, the Laplace transform of the terrestrial interference becomes analogous to (17), but this time the exclusion zone has a radius of length z.

When $A = b$, in addition to all the LTBSs, the aggregate interference includes also the power coming from the ABS (I_b) and therefore, on the same lines of [24, Eq. (51)], the additional factor is

$$\begin{aligned}\mathcal{I}_b(s) &= \mathbb{E}_{I_b}\left[e^{-s\,I_b}\right] \\ &= \mathbb{E}_{G_b}\left[\exp\left(-s\,G_b\,(r_u + h_A)^{-\frac{\alpha}{2}}\,\mathcal{P}_L(r_u,h_A)\right)\right] \\ &\overset{(a)}{=} \left(\frac{m}{m + \zeta\,s\,(r_u^2+h_A^2)^{-\frac{\alpha}{2}}\,\mathcal{P}_L(r_u,h_A)}\right)^m, \end{aligned} \tag{21}$$

where (a) follows from the moment generating function (MGF) of the gamma distribution [26, Appendix E]. ■

D. COVERAGE PROBABILITY

Having derived the mathematical expressions of the distance distributions, the association probabilities, and the Laplace transforms of the interference of interest, we can finally obtain the coverage probability in a Nakagami-m fading environment.

1) LOCAL COVERAGE

The following theorems will provide both the exact and approximate expressions of the coverage probability at a specific distance from the disaster epicenter.

Theorem 5: The probability of being under coverage when located at a specific radial distance r_u from the disaster epicenter is given as

$$P_{c|A} = \begin{cases} \int_0^{\infty} a_{\varrho}(y)\,p_{c,r}(y)\,f_Y(y)\,\mathrm{d}y \\ + \int_0^{\infty} a_{T|\varrho}(z)\,p_{c,T|\varrho}(z)\,f_Z(z)\,\mathrm{d}z \\ \mathcal{A}_b\,p_{c,b} + \int_0^{\infty} a_{T|b}(z)\,p_{c,T|b}(z)\,f_Z(z)\,\mathrm{d}z \end{cases},$$

where the first and second equations refer to the cases with $A = \varrho$ and $A = b$, respectively, and

$$p_{c,r}(y) = \sum_{k=0}^{m-1} \frac{\left(-m\,\mu_{\varrho}(y)\right)^k}{k!} \int_0^{\infty} \frac{\partial^k}{\partial s^k}\,\mathcal{L}_{\varrho}(s,y)\Big|_{s=\frac{m\,\mu_{\varrho}(y)}{g}} \times g^{-k}\,f_G(g)\,\mathrm{d}g \tag{22}$$

with $\mu_{\varrho}(y) = \frac{\theta}{M^2}\left(\left(r_u^2 + h_A^2\right)\left(y^2 + h_{AT}^2\right)\right)^{\frac{\alpha}{2}}$,

$$p_{c,b} = \sum_{k=0}^{m-1} \frac{(-m\,\mu_b)^k}{k!} \frac{\partial^k}{\partial s^k}\,\mathcal{L}_b(s)\Big|_{s=m\,\mu_b} \tag{23}$$

with $\mu_b = \theta\,\zeta^{-1}\,(r_u^2 + h_A^2)^{\frac{\alpha}{2}}$,

$$p_{c,T|\varrho}(z) = \sum_{k=0}^{m-1} \frac{(-m\,\mu_T(z))^k}{k!} \times \frac{\partial^k}{\partial s^k}\mathcal{L}_{T|\varrho}(s,z)\Big|_{s=m\,\mu_T(z)} \tag{24}$$

with $\mu_T(z) = \theta\,(z^2 + h_T^2)^{\frac{\alpha}{2}}$, and

$$p_{c,T|b}(z) = \sum_{k=0}^{m-1} \frac{(-m\,\mu_T(z))^k}{k!} \times \frac{\partial^k}{\partial s^k}\left(\mathcal{I}_b(s)\,\mathcal{L}_{T|b}(s,z)\right)\Big|_{s=m\,\mu_T(z)}. \tag{25}$$

Proof: See Appendix D.

Theorem 6: Let $\varepsilon = \mathbb{1}(m \le 1) + (m!)^{-\frac{1}{m}}\,\mathbb{1}(m > 1)$. Then, to ease the analytical evaluation of the coverage, the conditional coverage probabilities introduced in Theorem 5 can be

approximated as [24, Sec. III-D]

$$\begin{cases} p_{c,r}(y) \approx \sum_{k=1}^{m} \binom{m}{k} (-1)^{k+1} \\ \qquad \times \int_0^{\infty} \mathcal{L}_{\varrho}\left(\frac{k\,\varepsilon\, m\, \mu_{\varrho}(y)}{g}, y\right) f_G(g)\,\mathrm{d}g \\ p_{c,b} \approx \sum_{k=1}^{m} \binom{m}{k} (-1)^{k+1}\, \mathcal{L}_b(k\,\varepsilon\, m\, \mu_b) \\ p_{c,T|A}(z) \approx \sum_{k=1}^{m} \binom{m}{k} (-1)^{k+1}\, \mathcal{L}_{T|A}\left(k\,\varepsilon\, m\, \mu_T(z), z\right) \end{cases}.$$

Proof: See Appendix E. ■

2) AVERAGE COVERAGE

To have an overview of the network's performance, it is often preferable to compute the overall coverage over a certain area (perhaps while taking into account the users' distribution). Hence, the following theorem provides the expressions of the average coverage over the disaster-struck area.

Theorem 7: Given $A \in \{\varrho, b\}$ and noting that $P_{c|A} \equiv P_{c|A}(r_u)$, the expected value of the coverage probability over $\mathcal{A}_d$ is

$$\hat{P}_{c,d|A} = \int_0^{r_d} P_{c|A}(r_u)\, f_{R_u}(r_u)\,\mathrm{d}r_u, \tag{26}$$

where, in case of uniformly distributed users, $f_{R_u}(r_u) = 2r_u/r_d^2$.

Proof: The result follows from the integration of the coverage probability over the PDF of the RV R_u specified for the area of interest $\mathcal{A}_d$.

Alternatively, introducing $\lambda_u(r_u)$ as the users' density, $\hat{P}_{c,d|A}$ can be obtained as

$$\hat{P}_{c,d|A} = \frac{\int_0^{r_d} P_{c|A}(r_u)\, \lambda_u(r_u)\, r_u\,\mathrm{d}r_u}{\int_0^{r_d} \lambda_u(r_u)\, r_u\,\mathrm{d}r_u}, \tag{27}$$

which in case of uniform distribution ($\lambda_u = \text{const.}$) becomes

$$\hat{P}_{c,d|A} = \frac{2\,\lambda_u \int_0^{r_d} P_{c|A}(r_u)\, r_u\,\mathrm{d}r_u}{\lambda_u\, r_d^2} = \frac{2}{r_d^2}\int_0^{r_d} P_{c|A}(r_u)\, r_u\,\mathrm{d}r_u, \tag{28}$$

which is indeed equivalent to (26) when $f_{R_u}(r) = \frac{2r}{r_d^2}$. ■

IV. NUMERICAL RESULTS

The aim of this section is twofold: (i) verify the correctness of the mathematical framework we have developed and (ii) compare the performances of the post-disaster network without any ad hoc deployment, with the aid of an ARIS, or with the aid of an ABS. Therefore, we hereby show insightful results in terms of both the average and local coverage probabilities, depending on system parameters, such as: the UAV's communications-related power consumption [4] (henceforth intended for just relaying or reflecting signals), disaster radius r_d, distance from the disaster epicenter r_u, and UAV's altitude h_A. Moreover, we characterize the post-disaster network's performance depending on the type of environment, to which the s-curve parameters $\mathcal{S}$ and $\mathcal{S}'$, as well as the TBSs' altitude h_T and original density λ_0, are related.

To this extent, we perform Monte Carlo simulations and verify them analytically by applying the expressions derived in Section III; the results are depicted as solid lines for the simulation and markers for the analysis. Moreover, the main system parameters are set as in Table 2, unless differently stated; in particular, the standard value of the communications-related power consumption is set to 1 W based on the RIS prototype presented in [27], which consists of a board including 1100 elements and having an area of roughly a quarter of a meter square. Finally, note that the SINR threshold has been set at -5 dB since in emergency situations most of the required services are calls and text messages, which are much less data-hungry than other ordinary applications such as video streaming and gaming; nonetheless, the reader can refer to the coverage behaviors shown in [28, Figs. 2, 6, 7] to estimate the resulting coverage in case of a different value of SINR threshold.

A. UAV'S CHARACTERISTICS

In this subsection, we investigate the average coverage probability within a circular disaster-struck area of radius $r_d = 1$ km; in particular, we assume a linear relation between the RIS communications-related power consumption and its number of elements (therefore, if 1 W corresponds to $M = 1100$, then 0.1 W corresponds to $M = 110$, and so on), and consider the communications-related power consumption as the transmit power for the case where $A = b$. First of all, we should note from Fig. 2 that for the considered network parameters the coverage probability generally decreases as the urbanization level increases, since taller buildings lead to more obstructions in the desired communication links. However, for high-rise urban environments the average coverage provided by the terrestrial network alone is higher than its urban and dense urban counterparts (see the dashed lines); this can be explained by noting that the extremely high value of λ_0 ensures a short distance to the serving node, while a high percentage of potential interferers is obstructed by the buildings.

Our results show that the ARIS-aided architecture generally outperforms its ABS-aided counterpart. However, UAV's characteristics such as altitude and power consumption can play an important role in the overall network performance. These parameters should be set properly, since their effects are not independent: generally speaking, the altitude should be increased as the communications-related power consumption increases (although this is not always true for the ABS case), but a high altitude and a lower power (or vice versa) cannot ensure a good coverage. For example, the ARIS would lead to the maximum coverage when $h_A \to 1$ km (except for suburban environments, where the bottleneck is often represented by the path loss instead of the LoS probability), while the ABS should be deployed at significantly lower altitudes. This is

[4] Although the overall power consumption (essentially the power needed by the vehicle to fly and carry any equipment) is expected to be higher when the UAV carries an ABS, this and similar considerations go beyond the scope of our work.

TABLE 2. Main System Parameters (Sets' Elements Correspond to {Suburban, Urban, Dense Urban, High-Rise Urban} Environments)

Parameters	Values
Number of Monte Carlo iterations	5×10^4
Quality of resilience	$\chi(r) = \left(\frac{r}{r_d}\right)^2$
Path loss exponent for LoS transmission	$\alpha = 2.3$
Nakagami-m shape parameter for LoS transmission	$m = 3$
SINR threshold	$\theta = -5\,\text{dB} = 0.3162$
Original TBSs' density	$\lambda_0 = \{2, 4, 8, 16\}\,\text{TBSs/km}^2$
TBSs' altitude	$h_T = \{25, 30, 40, 60\}\,\text{m}$
UAV's altitude	$h_A = 500\,\text{m}$
UAV's communications-related power consumption	1 W
S-curve parameters	$\mathcal{S} = \{4.88, 9.612, 12.08, 27.23\}$ $\mathcal{S}' = \{0.429, 0.1581, 0.1139, 0.0797\}$

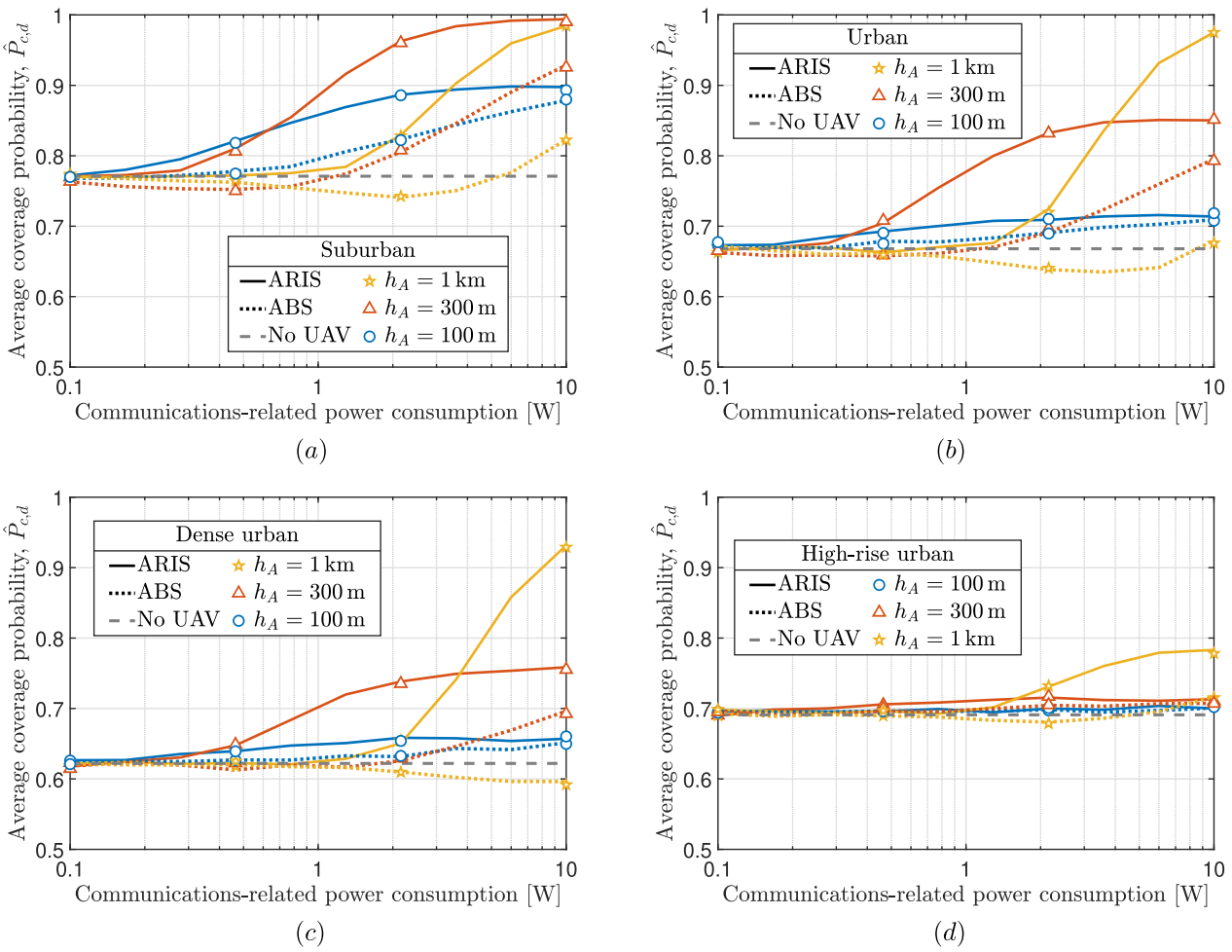

FIGURE 2. Average coverage probability within the disaster-struck area, as function of the communications-related power consumption and for various values of h_A, in a typical (*a*) suburban, (*b*) urban, (*c*) dense urban, or (*d*) high-rise urban environment.

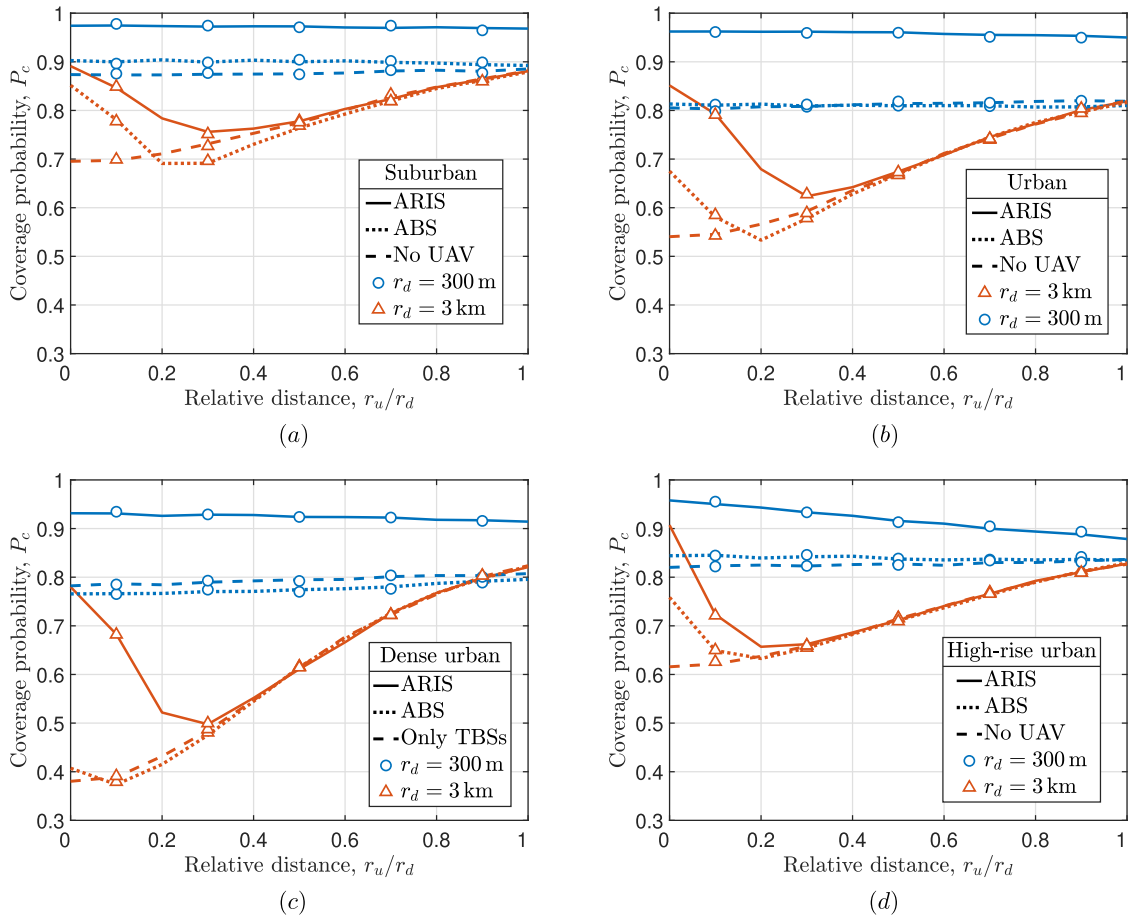

FIGURE 3. Local coverage probability, as function of the distance from the epicenter normalized on r_d for various values of r_d itself, in a typical (*a*) suburban, (*b*) urban, (*c*) dense urban, or (*d*) high-rise urban environment.

because, in contrast to the ARIS, the ABS can also act as an interferer, and affect the quality of service (QoS) experienced by the users far from the epicenter (which represent the majority); hence, a lower altitude allows the ABS to (positively) affect only its closeby users. Finally, we can note from Fig. 2(d) that the low LoS probability characterizing high-rise urban environments makes the overall impact of the UAV negligible, unless it carries an RIS with many antenna elements and at relatively high altitude.

B. NETWORK'S TOPOLOGY

Now, we locally compare the coverage probability as a function of the relative distance from the disaster epicenter. In particular, by inspecting Fig. 3 (which plots correspond to the four various types of environment described in [20]) we can notice the following similarities:

- No matter if the UAV is deployed or not, the coverage probability at the epicenter generally decreases as r_d increases;
- As we can see from the red curves, as r_u exceeds one kilometer the solid and the dotted lines rapidly converge, meaning that the influence of the considered ARIS or ABS has become negligible;
- For the TBS-only case, the minimum coverage within $\mathcal{A}_d$ occurs at the epicenter, while it occurs at a distance of approximately 600 or 900 m when the ABS or ARIS, respectively, is deployed.

  On the other hand, two important aspects depend on the environment's urbanization level:
- Consistently with Fig. 2, the impact of the disaster radius' value strongly depends on the urbanization level: generally speaking, as the latter increases the LoS probability decreases and consequently the network becomes more sensitive to r_d, except for high-rise urban environments;
- The higher the urbanization level, the milder the detrimental effect of the ABS when $r_d = 3$ km and $r_u/r_d \approx 0.2$.

V. SUMMARY AND FUTURE WORKS

In this article, we have presented a novel comparison between terrestrial-only, ABS-aided, and ARIS-aided post-disaster wireless networks, and proved that the latter generally outperforms the others, at least from a coverage perspective. To do so, a realistic but tractable system model (capturing aspects such as the QoR of the terrestrial network, size of the

disaster, user's location, type of environment, and UAV's characteristics) was devised and novel expressions of the distance distributions, association probabilities, Laplace transforms of the interference, and coverage probabilities were derived for any of the considered situations.

The most interesting extensions of this work are twofold: *(i)* the network model may be modified to take into account the possibility of deploying multiple ad hoc UAVs (which may be modeled as a BPP), while *(ii)* a more accurate performance analysis could be obtained by investigating also the SIR meta distribution (although this becomes challenging when considering Nakagami-m conditions).

APPENDIX A
PROOF OF THEOREM 1

The A-association probability is given by the joint probability that the UAV-UE link is in LoS condition and the average power received by the UE comes from the UAV instead of the closest LTBS. Thus, recalling that the UE's altitude is assumed negligible, we can write as follows:

$$\begin{aligned}
\mathcal{A}_{\varrho} &= \mathcal{P}_L(r_u, h_A)\,\mathbb{P}\left(\hat{q}_T(Z) < \hat{q}_{\varrho}(Y)\right) \\
&= \mathcal{P}_L(r_u, h_A)\,\mathbb{P}\Big((h_T^2 + Z^2)^{-\frac{\alpha}{2}} < M^2 \\
&\quad \times \left((r_u^2 + h_A^2)\,(Y^2 + h_{AT}^2)\right)^{-\frac{\alpha}{2}}\Big) \\
&= \mathcal{P}_L(r_u, h_A) \\
&\quad \times \mathbb{P}\left(h_T^2 + Z^2 \geq M^{-\frac{4}{\alpha}}\,(r_u^2 + h_A^2)\,(Y^2 + h_{AT}^2)\right) \\
&= \mathcal{P}_L(r_u, h_A) \\
&\quad \times \mathbb{P}\left(Z \geq \sqrt{M^{-\frac{4}{\alpha}}\,(r_u^2 + h_A^2)\,(Y^2 + h_{AT}^2) - h_T^2}\right) \\
&= \mathcal{P}_L(r_u, h_A) \int_0^{\infty} \bar{F}_Z\left(\mathcal{Z}_{\varrho}(y)\right)\, f_Y(y)\,\mathrm{d}y, \qquad (29)
\end{aligned}$$

with $\mathcal{Z}_{\varrho}(y) = \sqrt{M^{-\frac{4}{\alpha}}\,(r_u^2 + h_A^2)\,(y^2 + h_{AT}^2) - h_T^2}$. Now, by including the LoS probability term into the integral sign, we can introduce $a_{\varrho}(y) = \mathcal{P}_L(r_u, h_A)\,\bar{F}_Z(\mathcal{Z}_{\varrho}(y))$ as the corresponding conditional A-association probability.

On the other side, if the deployed UAV carries a BS equipment, with the same approach we obtain

$$\begin{aligned}
\mathcal{A}_b &= \mathcal{P}_L(r_u, h_A)\,\mathbb{P}\left(\hat{q}_T(Z) < \hat{q}_b\right) \\
&= \mathcal{P}_L(r_u, h_A)\,\mathbb{P}\left((h_T^2 + Z^2)^{-\frac{\alpha}{2}} < \zeta\,(h_A^2 + r_u^2)^{-\frac{\alpha}{2}}\right) \\
&= \mathcal{P}_L(r_u, h_A)\,\mathbb{P}\left(Z \geq \sqrt{\zeta^{-\frac{2}{\alpha}}\,(h_A^2 + r_u^2)^{-\frac{\alpha}{2}} - h_T^2}\right) \\
&= \mathcal{P}_L(r_u, h_A)\,\bar{F}_Z(\mathcal{Z}_b), \qquad (30)
\end{aligned}$$

with $\mathcal{Z}_b = \sqrt{\zeta^{-\frac{2}{\alpha}}\,(h_A^2 + r_u^2)^{-\frac{\alpha}{2}} - h_T^2}$.

APPENDIX B
PROOF OF THEOREM 2

By noting that the events 'the UAV is in NLoS with the UE' and 'the UAV is in LoS with the UE but the latter receives the strongest average power from an LTBS' are disjoint, we can compute the T-association probability as their sum.

Thus, assuming that the UAV carries an RIS (that is, $A = \varrho$), we can proceed as follows:

$$\begin{aligned}
\mathcal{A}_{T|\varrho} &= \mathcal{P}_L(r_u, h_A)\,\mathbb{P}\Big(\left(h_T^2 + Z^2\right)^{-\frac{\alpha}{2}} \geq M^2 \\
&\quad \times \left(\left(r_u^2 + h_A^2\right)\,\left(Y^2 + h_{AT}^2\right)\right)^{-\frac{\alpha}{2}}\Big) + \mathcal{P}_N(r_u, h_A) \\
&= \mathcal{P}_L(r_u, h_A)\,\mathbb{P}\Big(h_T^2 + Z^2 < M^{-\frac{4}{\alpha}} \\
&\quad \times \left(r_u^2 + h_A^2\right)\,\left(Y^2 + h_{AT}^2\right)\Big) + \mathcal{P}_N(r_u, h_A) \\
&= \mathcal{P}_L(r_u, h_A)\,\mathbb{P}\left(\frac{M^{\frac{4}{\alpha}}\,\left(h_T^2 + Z^2\right)}{r_u^2 + h_A^2} < Y^2 + h_{AT}^2\right) \\
&\quad + \mathcal{P}_N(r_u, h_A) \\
&= \mathcal{P}_L(r_u, h_A)\,\mathbb{P}\left(Y > \sqrt{\frac{M^{\frac{4}{\alpha}}\,\left(h_T^2 + Z^2\right)}{r_u^2 + h_A^2} - h_{AT}^2}\right) \\
&\quad + \mathcal{P}_N(r_u, h_A) \\
&= \mathcal{P}_L(r_u, h_A) \int_0^{\infty} \bar{F}_Y\left(\mathcal{Y}_{\varrho}(z)\right)\, f_Z(z)\,\mathrm{d}z + \mathcal{P}_{\mathrm{N}}(\mathrm{r_u}, \mathrm{h_A}), \qquad (31)
\end{aligned}$$

with $\mathcal{Y}_{\varrho}(z) = \sqrt{\frac{M^{\frac{4}{\alpha}}\,(h_T^2 + z^2)}{r_u^2 + h_A^2} - h_{AT}^2}$. Hence, $a_{T|\varrho}(z) = \mathcal{P}_L(r_u, h_A)\,\bar{F}_Y(\mathcal{Y}_{\varrho}(z)) + \mathcal{P}_N(r_u, h_A)$ defines the conditional T-association probability conditioned on the ARIS' deployment [5].

Similarly, when the UAV carries a BS ($A = b$) we can write

$$\begin{aligned}
\mathcal{A}_{T|b} &= \mathcal{P}_L(r_u, h_A)\,\mathbb{P}\left(\left(h_T^2 + Z^2\right)^{-\frac{\alpha}{2}} \geq \xi\,\left(r_u^2 + h_A^2\right)^{-\frac{\alpha}{2}}\right) \\
&\quad + \mathcal{P}_N(r_u, h_A) \\
&= \mathcal{P}_L(r_u, h_A)\,\mathbb{P}\left(Z < \sqrt{\xi^{-\frac{2}{\alpha}}\,\left(r_u^2 + h_A^2\right) - h_T^2}\right) \\
&\quad + \mathcal{P}_N(r_u, h_A) \\
&= \mathcal{P}_L(r_u, h_A)\,F_Z(\mathcal{Z}_b) + \mathcal{P}_N(r_u, h_A). \qquad (32)
\end{aligned}$$

Finally note that, in general, $\mathcal{A}_T = 1 - \mathcal{A}_A$.

[5] Recalling from (29) that $\hat{q}_T(Z) \geq \hat{q}_A(Y)$ implies $Z \leq \sqrt{M^{-\frac{4}{\alpha}}\,(r_u^2 + h_A^2)\,(Y^2 + h_{AT}^2) - h_T^2}$, an alternative way of computing the T-association probability would be $\mathcal{A}_{T|\varrho} = \int_0^{\infty} a'_{T|\varrho}(y)\, f_Y(y)\,\mathrm{d}y$, where $a'_{T|\varrho}(y) = \mathcal{P}_L(r_u, h_A)\,F_Z\left(\sqrt{M^{-\frac{4}{\alpha}}\,(r_u^2 + h_A^2)\,(y^2 + h_{AT}^2) - h_T^2}\right) + \mathcal{P}_N(r_u, h_A)$. While this expression is simpler than the previous one, it would lead to a more complicated expression of the coverage probability.

APPENDIX C
PROOF OF THEOREM 3

Let $\mathbf{W}$ denote the set of coordinates (from the UE's perspective) of the functioning TBSs. By introducing the function

$$\mathcal{I}_T(s,\omega) = 1 - \left(\frac{m}{m + s\left(\sqrt{\omega^2 + h_T^2}\right)^{-\alpha}} \right)^m, \tag{33}$$

the Laplace transform of the aggregate interference conditioned on the association to the ARIS can be derived by following the same approach of [29, Eq. (4), (16)]:

$$\begin{aligned}
\mathcal{L}_\varrho(s,y) &= \mathbb{E}\left[e^{-sI} \middle| B = r\right] \overset{(a)}{=} \mathbb{E}_\Phi\left[\prod_{W_i \in \check{\mathbf{\Phi}}} \psi(s, W_i)\right] \\
&\overset{(b)}{=} \exp\left(-\int_{\mathbb{R}^2 \setminus \mathcal{B}(\mathcal{Z}_\varrho(y))} \lambda_L(\|\mathbf{W}\|, h_T)\,(1 - \psi(s,\mathbf{W}))\,\mathrm{d}\mathbf{W}\right) \\
&= \exp\left(-\int_0^{2\pi}\int_{\mathcal{Z}_\varrho(y)}^{\infty} \lambda_L\left(r_\Omega(\check{\boldsymbol{\omega}},\beta)\right)\,\mathcal{I}_T(s,\check{\boldsymbol{\omega}})\,\check{\boldsymbol{\omega}}\,\mathrm{d}\check{\boldsymbol{\omega}}\,\mathrm{d}\beta\right),
\end{aligned} \tag{34}$$

where $\psi(s,W_i) = \mathbb{E}_{G_{W_i}}[\exp(-s\,G_{W_i}\,(\|W_i\|^2 + h_T^2)^{-\frac{\alpha}{2}})]$ and $\mathcal{B}(\mathcal{Z}_\varrho(y))$ is the ball representing the LTBSs' exclusion region around the UE (within such region there is no LTBS, otherwise the UE would have associated to one of them). Step (a) is due to the fact that the exponentially distributed gains G_{W_i}'s are independent from each other, whereas (b) follows by applying the probability generating functional (PGFL) to $\psi(s,W_i)$.

Also the expression of $\mathcal{L}_b(s)$ can be obtained by applying the same procedure.

APPENDIX D
PROOF OF THEOREM 5

Following the approach presented in [23, Sec. IV-D], when $A = \varrho$ the coverage probability can be computed as

$$\begin{aligned}
P_{c|r} &= \mathbb{E}_Y\left[a_\varrho(Y)\,p_{c,r}(Y)\right] + \mathbb{E}_Z\left[a_{T|\varrho}(Z)\,p_{c,T|\varrho}(Z)\right] \\
&= \int_0^\infty a_\varrho(y)\,p_{c,r}(y)\,f_Y(y)\,\mathrm{d}y \\
&\quad + \int_0^\infty a_{T|\varrho}(z)\,p_{c,T|\varrho}(z)\,f_Z(z)\,\mathrm{d}z,
\end{aligned} \tag{35}$$

while for $A = b$ it becomes

$$\begin{aligned}
P_{c|b} &= \mathcal{A}_b\,p_{c,b} + \mathbb{E}_Z\left[a_{T|b}(Z)\,p_{c,T|b}(Z)\right] \\
&= \mathcal{A}_b\,p_{c,b} + \int_0^\infty a_{T|b}(z)\,p_{c,T|b}(z)\,f_Z(z)\,\mathrm{d}z.
\end{aligned} \tag{36}$$

Therefore, in order to derive the exact expression of the respective coverage probabilities, we firstly have to derive the expressions of all the conditional coverage probabilities $p_{c,r}(y)$, $p_{c,b}$, $p_{c,T|\varrho}(z)$, and $p_{c,T|b}(z)$.

By introducing the function $\mu_\varrho(y) = \frac{\theta}{M^2}\left((r_u^2 + h_A^2)\,(y^2 + h_{AT}^2)\right)^{\frac{\alpha}{2}}$, the former will be

$$\begin{aligned}
p_{c,r}(y) &= \mathbb{P}\left(\frac{M^2\,G_\varrho\,\left(r_u^2 + h_A^2\right)^{-\frac{\alpha}{2}}\,G'_\varrho\,\left(y^2 + h_{AT}^2\right)^{-\frac{\alpha}{2}}}{I_T} > \theta\right) \\
&= \mathbb{P}\left(G_\varrho > \mu_\varrho(y)\,\frac{I_T}{G'_\varrho}\right),
\end{aligned}$$

which, recalling from [24, Appendix E] that $\bar{F}_G(g) = \frac{\Gamma_u(m,m\,g)}{\Gamma(m)} = \exp(-m\,g)\sum_{k=0}^{m-1}\frac{(m\,g)^k}{k!}$ and $\mathbb{E}_I[e^{-s\,I}\,I^k] = (-1)^k\,\frac{\partial^k}{\partial s^k}\mathcal{L}(s,y)$, can be rewritten as

$$\begin{aligned}
p_{c,r}(y) &= \mathbb{E}_{I_T,G'_\varrho}\left[\bar{F}_G\left(\mu_\varrho(y)\,\frac{I_T}{G'_\varrho}\right)\right] \\
&= \mathbb{E}_{I_T,G'_\varrho}\left[\exp\left(-m\,\mu_\varrho(y)\,\frac{I_T}{G'_\varrho}\right)\right. \\
&\quad \left.\times \sum_{k=0}^{m-1}\frac{\left(m\,\mu_\varrho(y)\,\frac{I_T}{G'_\varrho}\right)^k}{k!}\right] \\
&= \sum_{k=0}^{m-1}\mathbb{E}_{I_T,G'_\varrho}\left[\exp\left(-\frac{m\,\mu_\varrho(y)}{G'_\varrho}\,I_T\right)\left(\frac{I_T}{G'_\varrho}\right)^k\right] \\
&\quad \times \frac{\left(m\,\mu_\varrho(y)\right)^k}{k!} \\
&= \sum_{k=0}^{m-1}\int_0^\infty \mathbb{E}_{I_T}\left[\exp\left(-\frac{m\,\mu_\varrho(y)}{g}\,I_T\right)I_T^k\right]g^{-k} \\
&\quad \times f_G(g)\,\mathrm{d}g\,\frac{\left(\mathrm{m}\,\mu_\varrho(\mathrm{y})\right)^{\mathrm{k}}}{\mathrm{k!}} \\
&= \sum_{k=0}^{m-1}\frac{\left(-m\,\mu_\varrho(y)\right)^k}{k!} \\
&\quad \times \int_0^\infty \frac{\partial^k}{\partial s^k}\,\mathcal{L}_\varrho(s,y)\Big|_{s=\frac{m\,\mu_\varrho(y)}{g}}\,g^{-k}\,f_G(g)\,\mathrm{d}g.
\end{aligned} \tag{37}$$

Similarly, the coverage probability conditioned on the association to the ABS can be derived as

$$\begin{aligned}
p_{c,b} &= \mathbb{P}\left(\frac{\zeta\,G_b\,\left(r_u^2 + h_A^2\right)^{-\frac{\alpha}{2}}}{I_T} > \theta\right) = \mathbb{P}\left(G_b > \mu_b\,I_T\right) \\
&= \mathbb{E}_{I_T}\left[e^{-m\,\mu_b\,I_T}\sum_{k=0}^{m-1}\frac{(m\,\mu_b\,I_T)^k}{k!}\right] \\
&= \sum_{k=0}^{m-1}\mathbb{E}_{I_T}\left[e^{-m\,\mu_b\,I_T}\,I_T^k\right]\frac{(m\,\mu_b)^k}{k!}
\end{aligned}$$

$$= \sum_{k=0}^{m-1} \frac{(-m\,\mu_b)^k}{k!} \frac{\partial^k \mathcal{L}_b(s)}{\partial s^k}\bigg|_{s=m\,\mu_b}, \tag{38}$$

where $\mu_b = \theta\,\zeta^{-1}\,(r_u^2 + h_A^2)^{\frac{\alpha}{2}}$.

Finally, by introducing $\mu_T(z) = \theta\,(z^2 + h_T^2)^{\frac{\alpha}{2}}$, for the terrestrial components we will have

$$\begin{aligned} p_{c,T|\varrho}(z) &= \mathbb{P}\left(G_T > \mu_T(z)\,I_T\right) \\ &= \mathbb{E}_{I_T}\left[e^{-m\,\mu_T(z)\,I_T} \sum_{k=0}^{m-1} \frac{(m\,\mu_T(z)\,I_T)^k}{k!}\right] \\ &= \sum_{k=0}^{m-1} \frac{(-m\,\mu_T(z))^k}{k!} \frac{\partial^k \mathcal{L}_{T|\varrho}(s,z)}{\partial s^k}\bigg|_{s=m\,\mu_T(z)}, \end{aligned} \tag{39}$$

and,

$$\begin{aligned} p_{c,T|b}(z) &= \mathbb{P}\left(G_T > \mu_T(z)\,\left(\mathcal{P}_L(r_u,h_A)\,I_b + I_T\right)\right) \\ &= \sum_{k=0}^{m-1} \frac{(-m\,\mu_T(z))^k}{k!} \frac{\partial^k}{\partial s^k}\left(\mathcal{I}_b(s)\,\mathcal{L}_{T|b}(s,z)\right)\bigg|_{s=m\,\mu_T(z)}. \end{aligned} \tag{40}$$

APPENDIX E
PROOF OF THEOREM 6

Let us preliminarily introduce the lower incomplete Gamma function as

$$\Gamma_l(m, m\,g) = \int_0^{m\,g} t^{m-1}\,e^{-t}\,\mathrm{dt}, \tag{41}$$

which according to [30] can be bounded (and even approximated, according to [31]) as

$$\frac{\Gamma_l(m, m\,g)}{\Gamma(m)} \lessapprox \left(1 - e^{-\varepsilon\,m\,g}\right)^m, \tag{42}$$

where $\varepsilon = \mathbb{1}(m \le 1) + (m!)^{-\frac{1}{m}}\,\mathbb{1}(m > 1)$.

The coverage probability conditioned on the association to the ARIS can be approximated as follows: from the very first equality of (37) and recalling that $\bar{\boldsymbol{F}}_G(g) = \frac{\Gamma_u(m,\,m\,g)}{\Gamma(m)}$, we have

$$\begin{aligned} p_{c,r}(y) &= \mathbb{E}_{I_T,G'_\varrho}\left[\bar{\boldsymbol{F}}_G\left(\mu_\varrho(y)\,\frac{I_T}{G'_\varrho}\right)\right] \\ &= \mathbb{E}_{I_T,G'_\varrho}\left[\frac{\Gamma_u\left(m,\,m\,\mu_\varrho(y)\,\frac{I_T}{G'_\varrho}\right)}{\Gamma(m)}\right]. \end{aligned} \tag{43}$$

Now, recalling from [30] that $\frac{\Gamma_u(m,\,m\,n)}{\Gamma(m)} = 1 - \frac{\Gamma_l(m,\,m\,n)}{\Gamma(m)}$, we can rewrite

$$\begin{aligned} p_{c,r}(y) &= 1 - \mathbb{E}_{I_T,G'_\varrho}\left[\frac{\Gamma_l\left(m,\,m\,\mu_\varrho(y)\,\frac{I_T}{G'_\varrho}\right)}{\Gamma(m)}\right] \\ &\approx 1 - \mathbb{E}_{I_T,G'_\varrho}\left[\left(1 - \exp\left(-\varepsilon\,m\,\mu_\varrho(y)\,\frac{I_T}{G'_\varrho}\right)\right)^m\right] \\ &\overset{(a)}{=} \mathbb{E}_{I_T,G'_\varrho}\left[\sum_{k=1}^{m}\binom{m}{k}(-1)^{k+1} \times \exp\left(-k\,\varepsilon\,m\,\mu_\varrho(y)\,\frac{I_T}{G'_\varrho}\right)\right] \\ &= \sum_{k=1}^{m}\binom{m}{k}(-1)^{k+1} \times \mathbb{E}_{I_T,G'_\varrho}\left[\exp\left(-\frac{k\,\varepsilon\,m\,\mu_\varrho(y)}{G'_\varrho}\,I_T\right)\right] \\ &= \sum_{k=1}^{m}\binom{m}{k}(-1)^{k+1} \times \int_0^\infty \mathcal{L}_\varrho\left(\frac{k\,\varepsilon\,m\,\mu_\varrho(y)}{g}, y\right) f_G(g)\,\mathrm{dg}, \end{aligned} \tag{44}$$

where (a) follows from the binomial theorem, assuming that m is an integer number.

Similarly, the coverage probability given that the UE associates to the ABS is

$$\begin{aligned} p_{c,b} &= \mathbb{E}_{I_T}\left[\bar{\boldsymbol{F}}_G(\mu_b\,I_T)\right] = 1 - \mathbb{E}_{I_T}\left[\frac{\Gamma_l(m,\,m\,\mu_b\,I_T)}{\Gamma(m)}\right] \\ &\approx 1 - \mathbb{E}_{I_T}\left[\left(1 - \exp(-\varepsilon\,m\,\mu_b\,I_T)\right)^m\right] \\ &= \sum_{k=1}^{m}\binom{m}{k}(-1)^{k+1}\,\mathbb{E}_{I_T}\left[\exp(-k\,\varepsilon\,m\,\mu_b\,I_T)\right] \\ &= \sum_{k=1}^{m}\binom{m}{k}(-1)^{k+1}\,\mathcal{L}_b(k\,\varepsilon\,m\,\mu_b). \end{aligned} \tag{45}$$

Finally, both the corresponding coverage probabilities conditioned on the association to an LTBS can be expressed as

$$\begin{aligned} p_{c,T|A}(z) &= 1 - \mathbb{E}_{I_T}\left[\frac{\Gamma_l\left(m,\,m\,\mu_T(z)\,I_T\right)}{\Gamma(m)}\right] \\ &\approx 1 - \mathbb{E}_{I_T}\left[\left(1 - \exp\left(-\varepsilon\,m\,\mu_T(z)\,I_T\right)\right)^m\right] \\ &= \sum_{k=1}^{m}\binom{m}{k}(-1)^{k+1}\,\mathcal{L}_{T|A}\left(k\,\varepsilon\,m\,\mu_T(z), z\right). \end{aligned} \tag{46}$$

REFERENCES

[1] I. for Economics and P. (IEP), "Ecological threat register," 2020, Accessed: Nov. 30, 2022. [online]. Available: https://www.visionofhumanity.org/wp-content/uploads/2020/10/ETR_web-1.pdf

[2] reliefweb, "2021 disasters in numbers," 2021. Accessed: Nov. 30, 2022. [online]. Available: https://reliefweb.int/report/world/2021-disasters-numbers

[3] reliefweb, "Global terrorism index 2022," 2022. Accessed: Nov. 30, 2022. [online]. Available : https://reliefweb.int/report/world/global-terrorism-index-2022

[4] H. Niu et al., "Active RIS assisted rate-splitting multiple access network: Spectral and energy efficiency tradeoff," *IEEE J. Sel. Areas Commun.*, vol. 41, no. 5, pp. 1452–1467, May 2023.

[5] M. Matracia, N. Saeed, M. A. Kishk, and M.-S. Alouini, "Post-disaster communications: Enabling technologies, architectures, and open challenges," *IEEE Open J. Commun. Soc.*, vol. 3, pp. 1177–1205, 2022.

[6] M. Matracia, M. A. Kishk, and M.-S. Alouini, "Reliability in post-disaster networks: A novel interference mitigation strategy." [Online]. Available: https://www.techrxiv.org/articles/preprint/Reliability_in_Post-Disaster_Networks_A_Novel_Interference-Mitigation_Strategy/24233122/1

[7] S. Chakrabarti and S. Das, "Poisson point process-based network modelling and performance analysis of multi-hop D2D chain relay formation in heterogeneous wireless network," *Int. J. Commun. Netw. Distrib. Syst.*, vol. 22, no. 1, pp. 98–122, 2019.

[8] T. Sakano et al., "Bringing movable and deployable networks to disaster areas: Development and field test of MDRU," *IEEE Netw.*, vol. 30, no. 1, pp. 86–91, Jan./Feb. 2016.

[9] M. Y. Selim and A. E. Kamal, "Post-disaster 4G/5G network rehabilitation using drones: Solving battery and backhaul issues," in *IEEE Globecom Workshops (GC Wkshps)*, 2018, pp. 1–6.

[10] A. M. Hayajneh, S. A. R. Zaidi, D. C. McLernon, M. Di Renzo, and M. Ghogho, "Performance analysis of UAV enabled disaster recovery networks: A stochastic geometric framework based on cluster processes," *IEEE Access*, vol. 6, pp. 26215–26230, 2018.

[11] M. Matracia, M. A. Kishk, and M.-S. Alouini, "UAV-aided post-disaster cellular networks: A novel stochastic geometry approach," *IEEE Trans. Veh. Technol.*, vol. 72, no. 7, pp. 9406–9418, Jul. 2023.

[12] H. Lu, Y. Zeng, S. Jin, and R. Zhang, "Enabling panoramic full-angle reflection via aerial intelligent reflecting surface," in *Proc. IEEE Int. Conf. Commun. Workshops (ICC Workshops)*, 2020, pp. 1–6.

[13] E. M. Mohamed, S. Hashima, and K. Hatano, "Energy aware multi-armed bandit for millimeter wave-based UAV mounted RIS networks," *IEEE Wireless Commun. Lett.*, vol. 11, no. 6, pp. 1293–1297, Jun. 2022.

[14] R. Aziz and T. Girici, "Deployment of a UAV-mounted intelligent reflecting surface in the THz band," in *Proc. IEEE Int. Balkan Conf. Commun. Netw. (BalkanCom)*, 2022, pp. 168–172.

[15] N. Gao, S. Jin, X. Li, and M. Matthaiou, "Aerial RIS-assisted high altitude platform communications," *IEEE Wireless Commun. Lett.*, vol. 10, no. 10, pp. 2096–2100, Oct. 2021.

[16] W. Jaafar, L. Bariah, S. Muhaidat, and H. Yanikomeroglu, "Enhancing UAV-based public safety networks with reconfigurable intelligent surfaces," in *Intelligent Unmanned Air Vehicles Communications for Public Safety Networks*. Berlin, Germany: Springer, 2022, pp. 145–167.

[17] Y. Chen and W. Cheng, "Performance analysis of RIS-equipped-UAV based emergency wireless communications," in *Proc. IEEE Int. Conf. Commun.*, 2022, pp. 255–260.

[18] S. Alfattani et al., "Aerial platforms with reconfigurable smart surfaces for 5G and beyond," *IEEE Commun. Mag.*, vol. 59, no. 1, pp. 96–102, Jan. 2021.

[19] M. Matracia, M. A. Kishk, and M.-S. Alouini, "Coverage analysis for UAV-assisted cellular networks in rural areas," *IEEE Open J. Veh. Technol.*, vol. 2, pp. 194–206, 2021.

[20] A. Al-Hourani, S. Kandeepan, and S. Lardner, "Optimal LAP altitude for maximum coverage," *IEEE Wireless Commun. Lett.*, vol. 3, no. 6, pp. 569–572, Dec. 2014.

[21] M. Matracia, M. A. Kishk, and M.-S. Alouini, "Exploiting wind-turbine-mounted base stations to enhance rural connectivity," *IEEE Commun. Mag.*, vol. 59, no. 12, pp. 50–56, Dec. 2021.

[22] Q. Wu, S. Zhang, B. Zheng, C. You, and R. Zhang, "Intelligent reflecting surface-aided wireless communications: A tutorial," *IEEE Trans. Commun.*, vol. 69, no. 5, pp. 3313–3351, May 2021.

[23] B. Galkin, J. Kibilda, and L. A. DaSilva, "A stochastic model for UAV networks positioned above demand hotspots in urban environments," *IEEE Trans. Veh. Technol.*, vol. 68, no. 7, pp. 6985–6996, Jul. 2019.

[24] M. Alzenad and H. Yanikomeroglu, "Coverage and rate analysis for vertical heterogeneous networks (VHetNets)," *IEEE Trans. Wireless Commun.*, vol. 18, no. 12, pp. 5643–5657, Dec. 2019.

[25] J. G. Andrews, F. Baccelli, and R. K. Ganti, "A tractable approach to coverage and rate in cellular networks," *IEEE Trans. Commun.*, vol. 59, no. 11, pp. 3122–3134, Nov. 2011.

[26] V. V. Chetlur and H. S. Dhillon, "Downlink coverage analysis for a finite 3-D wireless network of unmanned aerial vehicles," *IEEE Trans. Commun.*, vol. 65, no. 10, pp. 4543–4558, Oct. 2017.

[27] X. Pei et al., "RIS-aided wireless communications: Prototyping, adaptive beamforming, and indoor/outdoor field trials," *IEEE Trans. Commun.*, vol. 69, no. 12, pp. 8627–8640, Dec. 2021.

[28] C. Saha, H. S. Dhillon, N. Miyoshi, and J. G. Andrews, "Unified analysis of HetNets using poisson cluster processes under max-power association," *IEEE Trans. Wireless Commun.*, vol. 18, no. 8, pp. 3797–3812, Aug. 2019.

[29] J. G. Andrews, A. K. Gupta, and H. S. Dhillon, "A primer on cellular network analysis using stochastic geometry," 2016, *arXiv:1604.03183*.

[30] H. Alzer, "On some inequalities for the incomplete gamma function," *Math. Computation*, vol. 66, no. 218, pp. 771–778, 1997.

[31] T. Bai and R. W. Heath, "Coverage and rate analysis for millimeter-wave cellular networks," *IEEE Trans. Wireless Commun.*, vol. 14, no. 2, pp. 1100–1114, Feb. 2015.

MAURILIO MATRACIA (Student Member, IEEE) received the M.Sc. degree in electrical engineering from the University of Palermo, Palermo, Italy, in 2019. He is currently a Doctoral Student with the Communication Theory Lab, King Abdullah University of Science and Technology (KAUST), Thuwal, Saudi Arabia. His experience with IEEE includes serving as a Reviewer for several journals and was the recipient of prizes at the *SusTech 2021 student poster* as well as *ComSoc EMEA Region – Internet for* All contests. His research focuses onSG, with a special focus on rural and emergency communications.

MUSTAFA A. KISHK (Member, IEEE) received the B.Sc. and M.Sc. degrees from Cairo University, Giza, Egypt, in 2013 and 2015, respectively and the Ph.D. degree from Virginia Tech, Blacksburg, VA, USA, in 2018, all in electrical engineering. He is an Assistant Professor with the Electronic Engineering Department, Maynooth University, Maynooth, Ireland. He was a Postdoctoral Research Fellow with the Communication Theory Laboratory, King Abdullah University of Science and Technology, Thuwal, Saudi Arabia. He currently serves as an Associate Editor with IEEE WIRELESS COMMUNICATION LETTERS. His research interests include stochastic geometry, UAV-enabled communication systems, and satellite-enabled communications. He was the recipient of the IEEE ComSoc Outstanding Young Researcher Award for Europe, Middle East, and Africa Region, in 2022. He was recognized as an Exemplary Reviewer by the IEEE COMMUNICATIONS LETTERS in 2020 and 2021.

MOHAMED-SLIM ALOUINI (Fellow, IEEE) was born in Tunis, Tunisia. He received the Ph.D. degree in electrical engineering from California Institute of Technology (Caltech), Pasadena, CA, USA, in 1998. He was a Faculty Member with the University of Minnesota, Minneapolis, MN, USA and Texas A&M University at Qatar, Doha, Qatar, before joining King Abdullah University of Science and Technology, Thuwal, Saudi Arabia, as a Professor of electrical engineering in 2009. His research interests include modeling, design, and performance analysis of wireless communication systems.